coatings

MDPI

Review

Metal-Doped TiO_2 Thin Film as an Electron Transfer Layer for Perovskite Solar Cells: A Review

Dewi Suriyani Che Halin [1,2,*], Ayu Wazira Azhari [3,4], Mohd Arif Anuar Mohd Salleh [1,2], Nur Izzati Muhammad Nadzri [1,2], Petrica Vizureanu [5,6], Mohd Mustafa Al Bakri Abdullah [1,2], Juyana A. Wahab [1,2] and Andrei Victor Sandu [5,7,8,*]

1 Center of Excellence Geopolymer and Green Technology, Universiti Malaysia Perlis, Arau 02600, Malaysia
2 Faculty of Chemical Engineering and Technology, Universiti Malaysia Perlis, Arau 02600, Malaysia
3 Faculty of Civil Engineering and Technology, Universiti Malaysia Perlis, Arau 02600, Malaysia
4 Center of Excellence, Water Research and Environmental Sustainability Growth, Universiti Malaysia Perlis, Arau 02600, Malaysia
5 Faculty of Materials Science and Engineering, Gheorghe Asachi Technical University of Iasi, Blvd. D. Mangeron 71, 700050 Iasi, Romania
6 Technical Sciences Academy of Romania, Dacia Blvd. 26, 030167 Bucharest, Romania
7 Romanian Inventors Forum, Str. Sf. P. Movila 3, 700089 Iasi, Romania
8 National Institute for Research and Development in Environmental Protection, INCDPM, Splaiul Independentei 294, 060031 Bucharest, Romania
* Correspondence: dewisuriyani@unimap.edu.my (D.S.C.H.); sav@tuiasi.ro (A.V.S.)

Abstract: The electron transfer layer (ETL) plays a vital role in achieving high-performance perovskite solar cells (PSCs). Titanium dioxide (TiO_2) is primarily utilised as the ETL since it is low-cost, chemically stable, and has the simplest thin-film preparation methods. However, TiO_2 is not an ideal ETL because it leads to low conductivity, conduction band mismatch, and unfavourable electron mobility. In addition, the exposure of TiO_2 to ultraviolet light induces the formation of oxygen vacancies at the surface. To overcome these issues, doping TiO_2 with various metal ions is favourable to improve the surface structure properties and electronic properties. This review focuses on the bulk modification of TiO_2 via doping with various metal ions concentrations to improve electrical and optical properties, charge carrier density, and interfacial electron–hole recombination, thus contributing to enhancing the power conversion efficiency (PCE) of the PSCs.

Keywords: TiO_2; bulk modification; electron transfer layer; metal doping; perovskite solar cells

check for updates

Citation: Che Halin, D.S.; Azhari, A.W.; Mohd Salleh, M.A.A.; Muhammad Nadzri, N.I.; Vizureanu, P.; Abdullah, M.M.A.B.; Wahab, J.A.; Sandu, A.V. Metal-Doped TiO_2 Thin Film as an Electron Transfer Layer for Perovskite Solar Cells: A Review. *Coatings* **2023**, *13*, 4. https://doi.org/10.3390/coatings13010004

Academic Editor: Torsten Brezesinski

Received: 21 October 2022
Revised: 13 December 2022
Accepted: 16 December 2022
Published: 20 December 2022

Copyright: © 2022 by the authors. Licensee MDPI, Basel, Switzerland. This article is an open access article distributed under the terms and conditions of the Creative Commons Attribution (CC BY) license (https://creativecommons.org/licenses/by/4.0/).

1. Introduction

Perovskite solar cells (PSCs) have been identified as one of the candidates for next-generation solar cell materials since their first debut in 2009 [1]. In the past decades, the world has seen tremendous technological advancement through interfacial [2–4], composition [5,6], and charge collection efficiency optimization [7], which has led to a significant increase in its efficiency. PSCs mainly consist of a perovskite layer sandwiched between an electron transport layer (ETL) and a hole transport layer (HTL) [8].

The ETL, also known as the electron extraction layer or electron collection layer, has recently piqued the interest of researchers working on PSCs. Although some studies have claimed that an ETL-free PSCs is possible in obtaining cell efficiency of up to 20% [9,10], most researchers still believe that the ETL is vital in facilitating an efficient electron collection and transportation between the perovskite layer and the electrodes [11–13]. The ETL promotes the transportation of photogenerated electrons that are extracted from the perovskite layer before being collected through the ohmic contact by the electrodes [14]. Furthermore, it is also important for eliminating electrical shunts between the transparent electrode and the perovskite layer [15].

Various metal oxides, such as TiO_2 [16–18], ZnO_2 [19], and SnO_2 [20,21], are used as ETL materials. Among these, TiO_2 is commonly used due to its simple device structure, high thermal stability, low cost, and high compatibility with flexible substrates [22–24]. However, insufficient charge separation at the interface between the perovskite layer has been one of the main issues with TiO_2 besides the low electron mobility and high surface defect density [25,26].

2. Perovskite Solar Cell (PSC) Structure

Solar energy is currently one of the most widely used energy sources to fulfil current and future energy needs, as it is renewable and eco-friendly. To harvest this unlimited energy source, solar photovoltaic technology consisting of cells produced from various materials is used. Amidst the varying materials, PSCs have shown rapid enhancement in power conversion efficiency (PCE) from a mere 3.8% to >20% in less than a decade [27]. Currently, the highest confirmed conversion efficiency reported is 25.7% by UNIST (Figure 1) [28]. This was mostly attributed to the high carrier mobility, great light absorbing capability, small exciton binding energy, and direct band gap [29–31].

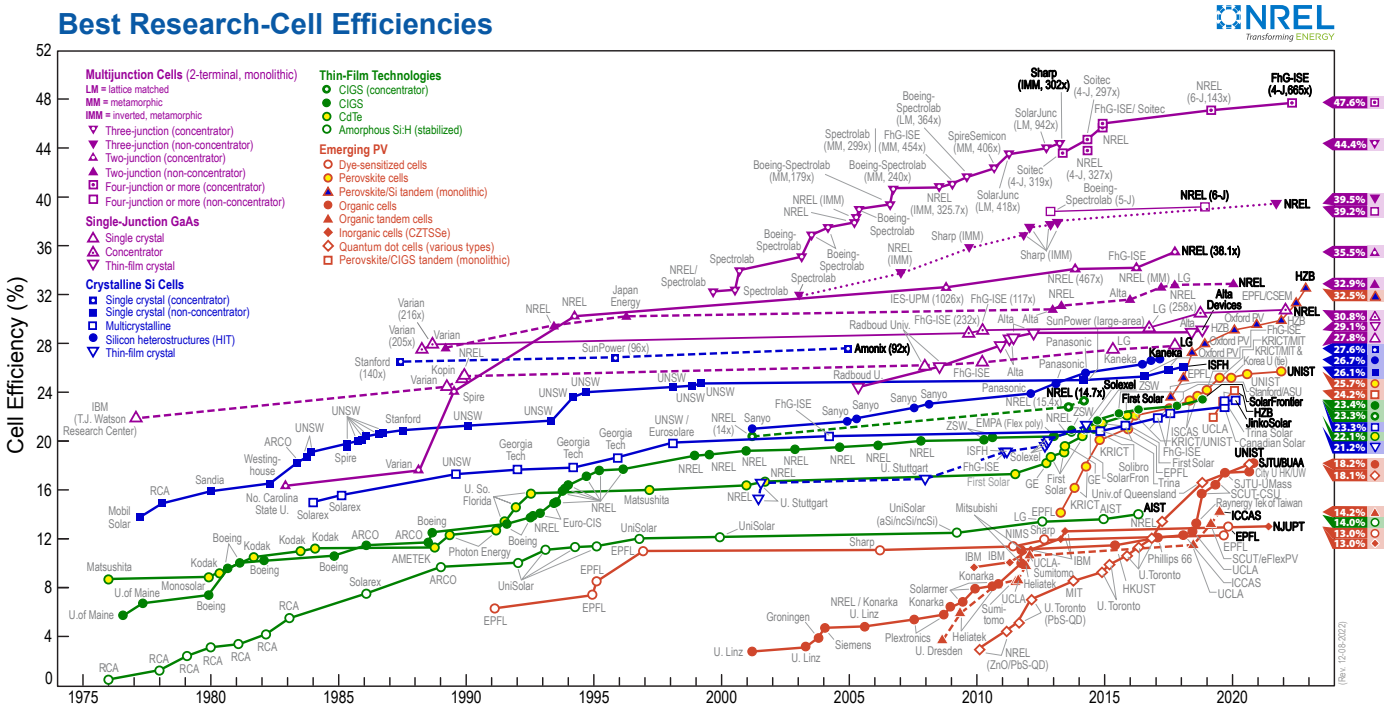


Figure 1. Best research cell efficiencies for various emerging solar photovoltaic materials. This plot is courtesy of the National Renewable Energy Laboratory, Golden, CO [28].

A standard PSC structure typically consists of multiple layers of thin films that include the conductive contact layer, hole transporting layer, perovskite as an absorber layer, an electron transport layer, and the substrate [32,33]. Figure 2 depicts the most common deposition sequence of a standard PSC. A fluorine- or indium-doped tin oxide is usually used as the substrate layer for the PSCs. The thin layer of ETL in this case, TiO_2, is first deposited on the cleaned substrate, followed by the deposition of the perovskite absorber layer. Another thin layer of hole-transporting material, for example, spiro-OMeTAD, is then deposited, and to complete the whole structure, a final layer of conductive contact is deposited. The layers are stacked together while ensuring that the band alignment of the heterojunction is in accordance with its distinct device configurations. Despite the device configurations, the incorporation of ETL seems to be the most effective way of improving the overall performance of PSCs [34,35].

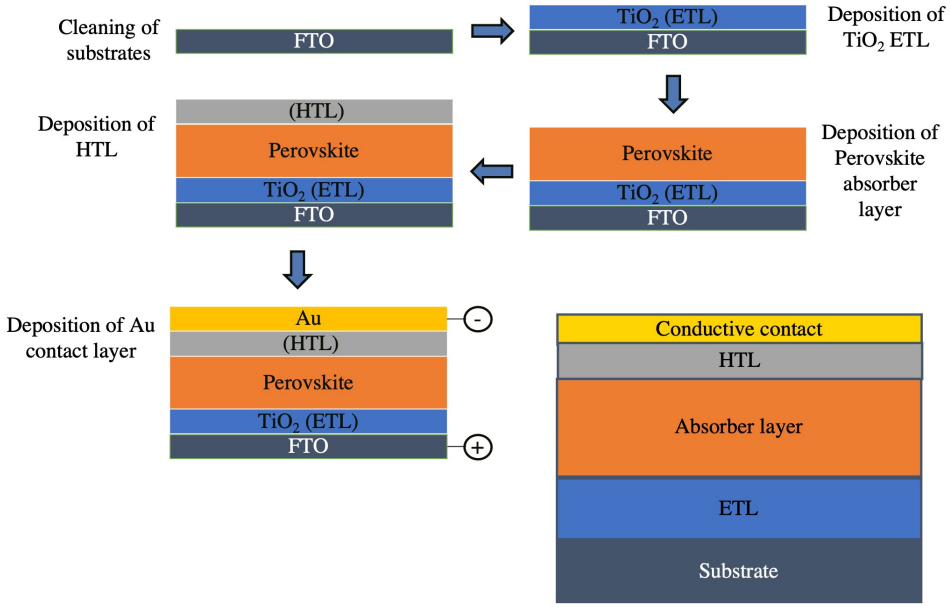


Figure 2. Sequential deposition of the layers in a typical PSC and standard PSC architecture.

A good structural and photoelectrochemical properties of an ETL can effectively expedite the whole electron collection and transfer process [36,37]. The manufacturing of a thin and dense ETL while ensuring a matching conduction band and good electron transfer properties results in a high-performance device. These characteristics reduce interfacial recombination while facilitating electron movement and charge accumulation [38–40].

3. Characteristics of ETL

Since PSCs were originally fabricated on solid-state dye-sensitised solar cells (DSSCs), a mesoporous TiO_2 scaffold structure was used (Figure 3c). However, due to the high-temperature process required for fabrication, a planar architecture (Figure 3a,b) similar to other thin-film solar cells is now common [41]. The characteristics of the ETL, including its energy level alignment, trap states, charge mobility and morphology-dependent parameters, material, and related interface properties, are vital for PSC performance [25,42]. When the energy level of the ETL/perovskite layer is matched, the electron extraction and transport properties are accelerated. This eventually increases the short-circuit current density (Jsc) and the fill factor (FF). The energy level is one of the important properties to ensure the improvement of the open-circuit voltage (V_{oc}) of a photovoltaic device. It can be determined by the energy level differences between the Fermi levels (EF) of the ETL and the EF of the hole-transporting layer (HTL). Figure 4 depicts the energy levels of various inorganic ETL materials. It is important to further investigate TiO_2 to develop a pathway to boost the PCE of perovskite solar cells via optimization, doping, and surface modification [23].

Various oxide metals have been widely used as ETLs, but most studies have shown that TiO_2 is the best one that can serve in both planar and mesoporous forms. Other oxide metals also have advantages but lack certain properties and need surface modification. Table 1 lists a comparison of TiO_2 with other oxide metals as an ETL.

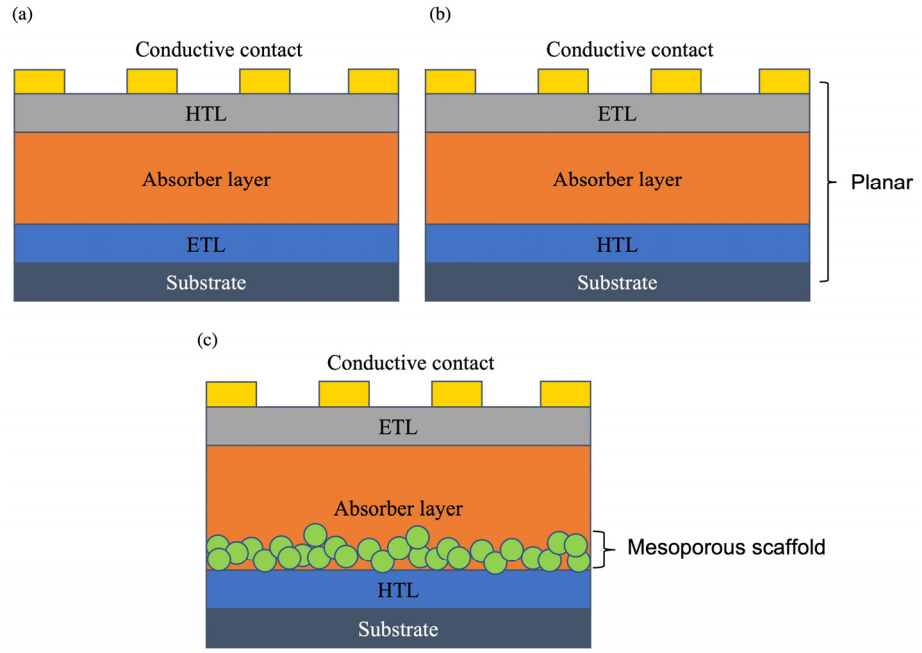


Figure 3. (**a**) Conventional PSC structure; (**b**) inverted PSC structure; (**c**) mesoporous PSC structure.

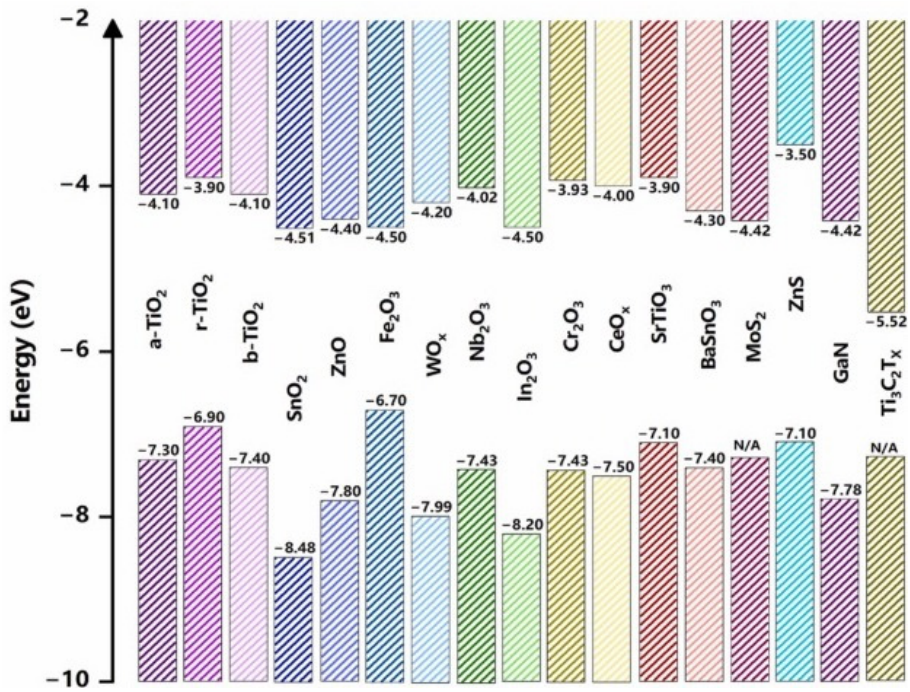


Figure 4. The energy levels of various inorganic ETLs. Reproduced with permission [14]. Copyright 2022, Elsevier.

Table 1. Comparison between TiO_2 and other oxide metals as electron transfer layers (ETLs) for perovskite solar cells (PSCs).

Oxide Metal	Comparison	References
TiO_2	• It has better hole-blocking properties, a suitable energy level match with the perovskite absorbing layer, and higher optical transparency. • A simple method for fabrication at a low cost. • The ability of electron transfer and long-time stability of PSCs. • A good photocatalyst material, and it is also widely used as an ETL for perovskite solar cells.	[43]
SnO_2	• SnO_2 has higher electron mobility, a deeper conduction band, and good transparency but less photocatalytic activity.	[44,45]
	• Negligible hysteresis has been produced in the devices with an SnO_2 ETL.	[46–48]
ZnO	• Has poor ZnO/perovskite interface chemical stability.	[49]
	• The large surface recombination, attributed to large surface defect concentrations, produces low fill factors and, consequently, lower efficiency. • The decomposition of perovskite deposited on ZnO during the process of annealing is attributed to the deprotonation of methyl ammonium in contact with ZnO, facilitated by the chemisorbed species on the surface.	[50]
WO_3	• The device produced is more sensitive to ambient moisture than TiO_2 under illumination. • Not commonly used as an ETL.	[51]
$Zn_2Ti_3O_8$, $BaSnO_3$, α-Fe_2O_3/PCBM	• These materials have not been extensively adopted, although in individual studies, these materials have exhibited improved performance over more conventional material choices. • Do not show clear advantages.	[52–54]

4. Titanium Dioxide (TiO_2) as an Electron Transfer Layer (ETL)

TiO_2 is an n-type semiconductor that can be formed into different polymorphs: anatase (tetragonal), brookite (orthorhombic), and rutile (tetragonal) [55,56]. The structural properties of different TiO_2 polymorphs are depicted in Table 2. TiO_2 in its pure form is not an ideal ETL due to drawbacks in several important criteria, including (a) low electron mobility (0.1–4 $cm^2v^{-1}s^{-1}$), which limits the effective electron transport [57]; (b) conduction band mismatch with compositional-tailored perovskite; (c) a high processing temperature of up to 450 °C [38]; (d) induction of the formation of oxygen vacancies at the surface when exposed to ultraviolet light [58]; and (e) high photocatalytic activity at the grain boundaries, which act as charge traps, resulting in the severe loss of photogenerated carriers through recombination and decomposition [59]. Thus, the interface between TiO_2 and perovskite retards the photoresponse of the resultant devices and leads to strong hysteresis [60].

Table 2. Structural properties of crystalline TiO_2 [56].

Properties	Crystalline Forms		
	Anatase	**Rutile**	**Brookite**
Crystalline structure	Tetragonal	Tetragonal	Rhombohedral
Lattice constants (nm)	$a = b = 0.3733$ $c = 0.9370$	$a = b = 0.4584$ $c = 0.2953$	$a = 0.5436$ $b = 0.9166$ $c = 0.5135$
Bravais lattice	Simple, body-centred	Simple, body-centred	Simple
Density (g/cm^{-3})	3.83	4.24	4.17
Melting point (°C)	Turning into rutile	1870	Turning into rutile
Boiling point (°C)	2927 [a]	-	-
Band gap (eV)	3.2	3.0	-
Refractive index (n)	2.5688	2.9467	2.8090
Standard heat capacity, Cp	55.52	55.60	-
Dielectric constant	55	110–117	78

[a] Pressure at pO_2 is 101.325 KPa. The italic a, b and c are the unit cell parameters.

Extensive research has been conducted to improve the bulk properties of TiO_2 ETLs, thus producing long-term stability of PSCs that include elemental doping [61,62], morphological control [63–65], and surface modification [66–69]. Surface modification is one way to produce a good-quality ETL by modulating the interface energetics and improving the physical contact between the ETL and the perovskite layer [70]. Both the layer thickness and morphology of the ETL can be controlled to ease electron extraction and transport, thus improving the optical properties of PSCs by inhibiting carrier recombination and promoting charge extraction [71].

The mesoporous morphology of the ETL surface can lead the perovskite material to enter the pores and cause a larger surface area of the perovskite layer [25]. In addition, direct contact between the perovskite absorbing layer and the contact layer can increase the recombination sites, causing a substantial loss of the photogenerated electron. In this case, morphological control is implemented by inserting photoanode materials between the perovskite material and the conductive contacts. By ensuring an appropriate band gap for the photoanode, it facilitates the electron transfer and hole-blocking of the contact simultaneously, suppressing the electron–hole recombination rate and enhancing the PCE of PSCs. [72]

Elemental doping involves the introduction of either a metal or non-metal dopant to improve the intrinsic properties of the TiO_2 layer. A wide range of elements has been used to dope TiO_2 to modify the light absorption, photocarrier bulk transportation, and surface transfer properties [73–75]. The incorporation of metal ions may have very little effect on the electron density; however, it helps improve the overall properties of the ETL by modulating the energy level, improving the electron dynamics, and decreasing the defect density [23].

5. Modification of TiO_2 with Metal Doping

Among the various methods used to enhance the bulk properties of TiO_2 ETLs, doping with metals ions has received much attention, as it is a simple process that can lead to improved charge transportation ability, elimination of hysteresis, modification of the band structure, modulated electron mobility, and improved thin film conductivity of the ETL with a high charge extraction capacity [76,77]. The numerous metal dopants that have been reported include tin [42,78,79], iron [80], ruthenium [81,82], sulphur [83,84], niobium [85], zinc [86], tantalum [87], and magnesium [77,88].

For instance, Su et al. (2019) reported that Sn-doped TiO_2 prepared by the co-electrodeposition method considerably improved the photovoltaic performance of PSCs by increasing the carrier concentration and enhancing the electron extraction capability

(Figure 5a,b). This was shown by the increase in the efficiency from 15.3% using pure TiO_2 to 16.8% when doped with Sn [78]. Another study by Wu et al. (2019) showed that gradient doping of Sn^{4+} on a compact TiO_2 ETL resulted in a high efficiency of 17.2% owing to the formation of a built-in electric field perpendicular to the substrate, which accelerated electron migration and reduced the charge recombination of the photocarriers and the transfer barrier (Figure 5c) [79]. Gradient doping is a rational way to maximize the photon-to-current efficiency of a photoelectrode. The gradient doping forms a homojunction from the top to the bottom of the perovskite film with a built-in field that facilitates the extraction of photogenerated carriers, resulting in an increased carrier extraction length. In particular, Deng et al. (2020) successfully attained a slightly better performance (17.77%) in the efficiency of the PSCs by passivation of hydriodic acid (HI) in the preparation of Sn-doped TiO_2. The results showed perfect alignment of the conduction band with the adjacent perovskite layer (Figure 5d) and the reduction of the defect density at the interface and in the entire film [89]. Koech et al. (2021) also reported that an increase of 7.16% PCE was attained in an SnO_2-doped TiO_2 ETL structure, resulting in an average PCE of 17.35% ± 1.39% as the result of improved electron extraction and transport ability [90].

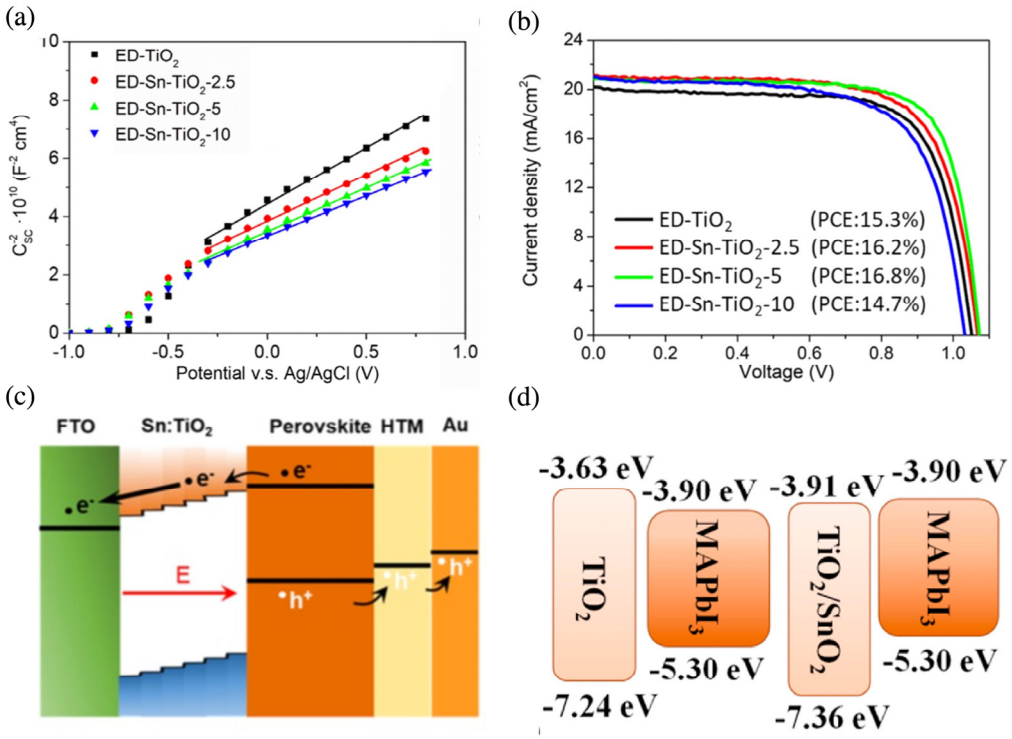


Figure 5. (**a**) The Mott–Schottky plots of pure ED-TiO_2 and various molar ratios of ED-Sn-TiO_2. (**b**) The highest-performing PSCs with pure and Sn-doped TiO_2. Reproduced with permission [78]. Copyright 2019, Wiley-VCH. (**c**) Schematic of energy level diagrams of PSCs based on the as-prepared TiO_2 ESL and thermally treated TiO_2 ESL. Reprinted (adapted) with permission from [79]. Copyright (2019) American Chemical Society. (**d**) Schematic diagram of band alignment for TiO_2/$MAPbI_3$ and TiO_2/SnO_2/$MAPbI_3$. Reproduced with permission [89]. Copyright 2020, Elsevier.

A previous study by Gu et al. (2017) reported the doping of Fe^{3+} into TiO_2 to improve the conductivity of TiO_2 compact layers and finally boost the performance of PSCs to attain an efficiency of 18.6%. The Fe^{3+}-doped TiO_2 solution was synthesized using a sol–gel method by mixing $Fe(NO_3)_3$ at different concentrations The results demonstrated that the conductivity was increased significantly due to the reduction in the electron trap density by the substitution of Fe^{3+} at the Ti^{3+} sites, which effectively passivated the oxygen vacancy defects in the TiO_2 compact layer [80]. A simulation study was conducted by Mulyanti et al. (2022), which showed that the absorption spectra of the Fe-doped TiO_2 increased to up to

81.7% by the manipulation of the ETL thickness. It was revealed that the absorption spectra fluctuated more for thicker ETLs, while thinner ETLs resulted in the spectra dropping at short wavelengths [91].

Among others, ruthenium (Ru) can also be used as a doping material, as it has an ionic radius comparable to that of Ti^{4+} (0.062 nm and 0.061 nm, respectively). Ti^{4+} can be replaced by Ru^{4+} without any strain or secondary phases. Wang et al. (2018), reported on the introduction of Ru ions into the compact layer of TiO_2 using the sol–gel spin coating technique to improve the properties of the ETL thin film. The titanium precursor solutions were prepared by mixing titanium diisopropoxide bis (acetylacetonate) solution in ethanol at a 1:10 vol ratio, followed by the addition of $RuCl_3$. Different concentrations of Ru^{4+} ions (0 mol%, 0.5 mol%, 1 mol%, 2 mol%, and 5 mol%) were used for the doped films. It was found that the density of the electron traps decreased dramatically without showing a negative effect on the optical properties. The results showed that at a concentration of 1 mol% Ru^{4+}, Ru-TiO_2-based solar cells revealed the highest efficiency of 18.35%, with improvement in carrier density and conductivity compared with pure TiO_2 owing to the matching band gap with a low resistivity, which affected the fill factor (FF) and open-circuit voltage (V_{oc}) of the device. The reduction in the excessive charge accumulation eventually resulted in increased FF and V_{oc} while promoting effective electron injection between the TiO_2 compact layer and the perovskite interface, thus increasing the overall performance of the PSCs [82]. In another study by Xu et al. (2018), a one-step spray pyrolysis technique was implemented in the doping of TiO_2 with Ru. It was found that the conductivity of Ru-doped TiO_2 was improved compared with using pure TiO_2, as shown by the enhanced photovoltaic performance of the PSCs [81].

Sulphur (S)-doped TiO_2 has been demonstrated to enhance photocurrent, light absorbance, and photocatalytic activity as well as modify the band gap energy in other applications, such as coatings and photocatalysis [83,92]. However, very few works have reported on using S as a dopant for TiO_2. Abd Mutalib et al. (2022) reported on the use of an S-doped TiO_2 ETL in the planar PSCs by using a modified sol–gel method. The S-doped TiO_2 ETL was prepared by mixing of 1.2 mL of acetyl acetone with 7 mL of titanium isopropoxide (TTIP), 35 mL absolute ethanol, and varied concentrations of thiourea (5 mol%, 10 mol%, and 15 mol%.) as the sulphur source. The final solution was then stirred for 180 min to produce a transparent and homogeneous solution. The produced S-doped TiO_2 showed high absorbance, photocatalytic activity, and photo-current density. This proved that the increase in the electron collection capacity of the carrier charge and photocurrent density enhanced the PCE by 6.0% and showed a better efficiency of 18%, as shown in Table 3 [84]. It showed that the charge transfer resistance (RCT) in the S-doped TiO_2 perovskite device was lower than that of the un-doped TiO_2 device. The lower resistance could facilitate higher electron transfer in the perovskite device, resulting in a higher overall PCE and finally enhancing the performance of the PSCs.

Table 3. The photocurrent–voltage (J–V) measurements for perovskite solar cell device using S-doped TiO_2 and un-doped TiO_2 with a 0.07 cm^2 active area [84].

Material	J_{sc} (mA/cm^2)	V_{oc} (V)	FF (%)	PCE (%)	R_{ct} (Ω)
TiO_2	13.30	0.98	39.88	5.10	18.72
-	13.18 ± 0.08	0.97 ± 0.01	38.70 ± 0.77	4.98 ± 0.13	20.68 ± 1.54
S-doped TiO_2	13.9	0.997	43.18	6.0	14.26
-	13.65 ± 0.17	0.99 ± 0.003	42.19 ± 0.83	5.76 ± 0.19	14.68 ± 1.05

Bidaki et al. (2022) studied niobium (Nb) doping into compact and mesoporous TiO_2 ETLs. A simple sol–gel spin coating process was used to deposit the parent solution of Nb-doped TiO_2 sol on the FTO/TiO_2-bl substrate, and $NbCl_5$ was used as the source of Nb. During the mixing process, the amount of $NbCl_5$ added into the parent solution varied from 0 to 5 at. % of Nb. The obtained films were characterized, and it was found that at higher visible light transmittances, greater charge transfer conductivities, and higher

Nb incorporation efficiencies, the compact layer ETL demonstrated superior performance compared with its mesoporous counterpart. The results showed that the doping of 5 at. % Nb into the compact TiO_2 ETL produced higher PCE compared with the mesoporous TiO_2 ETL, with 33.1% and 28.8% for the compact and mesoporous ETLs, respectively. The higher carrier injection with higher Nb incorporation efficiency produced during the addition of Nb to the TiO_2 crystal structure provided a band gap reduction in the ETL, which gave more potential between the conduction band of the perovskite layer and the conduction band of the TiO_2 ETL layer [93].

Overall, it has been confirmed that the bulk modification of TiO_2 by doping with different metal ions is an effective way to reduce the band gap and provide control of the electronic properties as well as the trap states of ETL. This results in an increased charge carrier density in the absorbing layer and improved electron transportation from the ETL to the conductive oxide substrate. The ion migration initiated by the illumination-induced electric field can be hindered or even stopped by the passivation of the grain boundaries in the device, which can decrease the packing density of the crystal lattice [94,95]. Metal doping can also lower the density of recombination hubs correlated with under-coordinated atoms, and the modification of the ETL/perovskite interface plays a role in facilitating the charge transport and the suppression of hysteresis and interfacial recombination to realize highly efficient and stable PSCs [96].

6. Conclusions

In the construction of PSCs, it is believed that the ETL is still a key player to ensure the good performance of the PSCs. This review covers the use of TiO_2 as an ETL and the characteristics of TiO_2 ETLs as well as their issues and drawbacks. Several metal-doping materials were discussed, focusing on the improvement of the bulk properties of the doped TiO_2 ETL, which include the modification of the electric structure and intrinsic properties, the improvement of the electrical conductivity by increasing the carrier density and mobility, and the modification of the bandgap alignments and interface trap density and distribution. It is believed that more studies should be conducted focusing on the availability of the materials, the simplicity and flexibility of the method, and the environmental impact of the overall process.

Author Contributions: Conceptualization, D.S.C.H. and M.A.A.M.S.; introduction, N.I.M.N. and A.W.A.; methodology and validation, D.S.C.H., P.V., A.W.A., A.V.S., M.A.A.M.S. and J.A.W.; resources, M.M.A.B.A., N.I.M.N. and J.A.W.; writing—original draft preparation, D.S.C.H.; writing—review and editing, D.S.C.H., M.M.A.B.A., A.W.A. and A.V.S. All authors have read and agreed to the published version of the manuscript.

Funding: This research publication was supported by the Gheorghe Asachi Technical University of Iasi (TUIASI) from the University Scientific Research Fund (FCSU).

Institutional Review Board Statement: Not applicable.

Informed Consent Statement: Not applicable.

Data Availability Statement: The data presented in this study are available in this review.

Acknowledgments: The authors would like to acknowledge the support from the Fundamental Research Grant Scheme under grant number FRGS/1/2021/TK0/UNIMAP/02/49 from the Ministry of Education Malaysia, the Center of Excellence Geopolymer & Green Technology (CEGeoGTech), and the Faculty of Chemical Engineering and Technology, Universiti Malaysia Perlis (UniMAP) for their partial support.

Conflicts of Interest: The authors declare no conflict of interest.

References

1. Kojima, A.; Teshima, K.; Shirai, Y.; Miyasaka, T. Organometal Halide Perovskites as Visible-Light Sensitizers for Photovoltaic Cells. *J. Am. Chem. Soc.* **2009**, *131*, 6050–6051. [CrossRef] [PubMed]

2. Xiang, W.; Liu, S.; Tress, W. Interfaces and Interfacial Layers in Inorganic Perovskite Solar Cells. *Angew. Chem. Int. Ed.* **2021**, *60*, 26440–26453. [CrossRef] [PubMed]
3. Zou, H.; Duan, Y.; Yang, S.; Xu, D.; Yang, L.; Cui, J.; Zhou, H.; Wu, M.; Wang, J.; Lei, X.; et al. 20.67%-Efficiency Inorganic $CsPbI_3$ Solar Cells Enabled by Zwitterion Ion Interface Treatment. *Small* **2022**, 2206205. [CrossRef] [PubMed]
4. Kumar, A.; Singh, S.; Sharma, A.; Ahmed, E.M. Efficient and stable perovskite solar cells by interface engineering at the interface of electron transport layer/perovskite. *Opt. Mater.* **2022**, *132*, 112846. [CrossRef]
5. Lu, H.; Krishna, A.; Zakeeruddin, S.M.; Grätzel, M.; Hagfeldt, A. Compositional and Interface Engineering of Organic-Inorganic Lead Halide Perovskite Solar Cells. *iScience* **2020**, *23*, 101359. [CrossRef]
6. Tian, J.; Wang, J.; Xue, Q.; Niu, T.; Yan, L.; Zhu, Z.; Li, N.; Brabec, C.J.; Yip, H.-L.; Cao, Y. Composition Engineering of All-Inorganic Perovskite Film for Efficient and Operationally Stable Solar Cells. *Adv. Funct. Mater.* **2020**, *30*, 2001764. [CrossRef]
7. Yoo, J.J.; Seo, G.; Chua, M.R.; Park, T.G.; Lu, Y.; Rotermund, F.; Kim, Y.-K.; Moon, C.S.; Jeon, N.J.; Correa-Baena, J.-P.; et al. Efficient perovskite solar cells via improved carrier management. *Nature* **2021**, *590*, 587–593. [CrossRef]
8. Mohamad Noh, M.F.; Teh, C.H.; Daik, R.; Lim, E.L.; Yap, C.C.; Ibrahim, M.A.; Ahmad Ludin, N.; Mohd Yusoff, A.R.b.; Jang, J.; Mat Teridi, M.A. The architecture of the electron transport layer for a perovskite solar cell. *J. Mater. Chem. C* **2018**, *6*, 682–712. [CrossRef]
9. Sadegh, F.; Akman, E.; Prochowicz, D.; Tavakoli, M.M.; Yadav, P.; Akin, S. Facile NaF Treatment Achieves 20% Efficient ETL-Free Perovskite Solar Cells. *ACS Appl. Mater. Interfaces* **2022**, *14*, 38631–38641. [CrossRef]
10. Gao, L.; Xu, C.; Su, Y.; Liu, A.; Ma, T. Cascaded band gap design for highly efficient electron transport layer-free perovskite solar cells. *Chem. Commun.* **2022**, *58*, 6749–6752. [CrossRef]
11. Huang, S.; Li, P.; Wang, J.; Huang, J.C.-C.; Xue, Q.; Fu, N. Modification of SnO_2 electron transport Layer: Brilliant strategies to make perovskite solar cells stronger. *Chem. Eng. J.* **2022**, *439*, 135687. [CrossRef]
12. Aftab, A.; Ahmad, M.I. A review of stability and progress in tin halide perovskite solar cell. *Sol. Energy* **2021**, *216*, 26–47. [CrossRef]
13. Kim, T.; Lim, J.; Song, S. Recent Progress and Challenges of Electron Transport Layers in Organic–Inorganic Perovskite Solar Cells. *Energies* **2020**, *13*, 5572. [CrossRef]
14. Zhang, T.; He, Q.; Yu, J.; Chen, A.; Zhang, Z.; Pan, J. Recent progress in improving strategies of inorganic electron transport layers for perovskite solar cells. *Nano Energy* **2022**, *104*, 107918. [CrossRef]
15. Prochowicz, D.; Tavakoli, M.M.; Wolska-Pietkiewicz, M.; Jędrzejewska, M.; Trivedi, S.; Kumar, M.; Zakeeruddin, S.M.; Lewiński, J.; Graetzel, M.; Yadav, P. Suppressing recombination in perovskite solar cells via surface engineering of TiO_2 ETL. *Sol. Energy* **2020**, *197*, 50–57. [CrossRef]
16. Zhao, Y.; Zhang, H.; Ren, X.; Zhu, H.L.; Huang, Z.; Ye, F.; Ouyang, D.; Cheah, K.W.; Jen, A.K.Y.; Choy, W.C.H. Thick TiO_2-Based Top Electron Transport Layer on Perovskite for Highly Efficient and Stable Solar Cells. *ACS Energy Lett.* **2018**, *3*, 2891–2898. [CrossRef]
17. Sławek, A.; Starowicz, Z.; Lipiński, M. The Influence of the Thickness of Compact TiO_2 Electron Transport Layer on the Performance of Planar CH3NH3PbI3 Perovskite Solar Cells. *Materials* **2021**, *14*, 3295. [CrossRef]
18. Han, G.S.; Chung, H.S.; Kim, B.J.; Kim, D.H.; Lee, J.W.; Swain, B.S.; Mahmood, K.; Yoo, J.S.; Park, N.-G.; Lee, J.H.; et al. Retarding charge recombination in perovskite solar cells using ultrathin MgO-coated TiO_2 nanoparticulate films. *J. Mater. Chem. A* **2015**, *3*, 9160–9164. [CrossRef]
19. Niu, H.; Fang, C.; Wei, X.; Wang, H.; Wan, L.; Li, Y.; Mao, X.; Xu, J.; Zhou, R. Magnetron sputtered ZnO electron transporting layers for high performance perovskite solar cells. *Dalton Trans.* **2021**, *50*, 6477–6487. [CrossRef]
20. Uddin, A.; Yi, H. Progress and Challenges of SnO_2 Electron Transport Layer for Perovskite Solar Cells: A Critical Review. *Sol. RRL* **2022**, *6*, 2100983. [CrossRef]
21. Jiang, Q.; Zhang, X.; You, J. SnO_2: A Wonderful Electron Transport Layer for Perovskite Solar Cells. *Small* **2018**, *14*, 1801154. [CrossRef] [PubMed]
22. Hu, W.; Zhou, W.; Lei, X.; Zhou, P.; Zhang, M.; Chen, T.; Zeng, H.; Zhu, J.; Dai, S.; Yang, S.; et al. Low-Temperature In Situ Amino Functionalization of TiO2 Nanoparticles Sharpens Electron Management Achieving over 21% Efficient Planar Perovskite Solar Cells. *Adv. Mater.* **2019**, *31*, 1806095. [CrossRef] [PubMed]
23. Zhen, C.; Wu, T.; Chen, R.; Wang, L.; Liu, G.; Cheng, H.-M. Strategies for Modifying TiO_2 Based Electron Transport Layers to Boost Perovskite Solar Cells. *ACS Sustain. Chem. Eng.* **2019**, *7*, 4586–4618. [CrossRef]
24. Yan, Y.; Liu, C.; Yang, Y.; Hu, G.; Tiwari, V.; Jiang, D.-E.; Peng, W.; Jha, A.; Duan, H.-G.; Tellkamp, F.; et al. Fundamental Flaw in the Current Construction of the TiO_2 Electron Transport Layer of Perovskite Solar Cells and Its Elimination. *ACS Appl. Mater. Interfaces* **2021**, *13*, 39371–39378. [CrossRef] [PubMed]
25. Yang, G.; Tao, H.; Qin, P.; Ke, W.; Fang, G. Recent progress in electron transport layers for efficient perovskite solar cells. *J. Mater. Chem. A* **2016**, *4*, 3970–3990. [CrossRef]
26. Jena, A.K.; Kulkarni, A.; Miyasaka, T. Halide Perovskite Photovoltaics: Background, Status, and Future Prospects. *Chem. Rev.* **2019**, *119*, 3036–3103. [CrossRef]
27. Chen, W.; Wu, Y.; Yue, Y.; Liu, J.; Zhang, W.; Yang, X.; Chen, H.; Bi, E.; Ashraful, I.; Grätzel, M.; et al. Efficient and stable large-area perovskite solar cells with inorganic charge extraction layers. *Science* **2015**, *350*, 944–948. [CrossRef]

28. Best Research-Cell Efficiency Chart. Available online: https://www.nrel.gov/pv/cell-efficiency.html (accessed on 3 December 2022).
29. Hwang, I.; Jeong, I.; Lee, J.; Ko, M.J.; Yong, K. Enhancing Stability of Perovskite Solar Cells to Moisture by the Facile Hydrophobic Passivation. *ACS Appl. Mater. Interfaces* **2015**, *7*, 17330–17336. [CrossRef]
30. Chang, C.-Y.; Chu, C.-Y.; Huang, Y.-C.; Huang, C.-W.; Chang, S.-Y.; Chen, C.-A.; Chao, C.-Y.; Su, W.-F. Tuning Perovskite Morphology by Polymer Additive for High Efficiency Solar Cell. *ACS Appl. Mater. Interfaces* **2015**, *7*, 4955–4961. [CrossRef]
31. Valadi, K.; Gharibi, S.; Taheri-Ledari, R.; Akin, S.; Maleki, A.; Shalan, A.E. Metal oxide electron transport materials for perovskite solar cells: A review. *Environ. Chem. Lett.* **2021**, *19*, 2185–2207. [CrossRef]
32. Malinkiewicz, O.; Yella, A.; Lee, Y.H.; Espallargas, G.M.; Graetzel, M.; Nazeeruddin, M.K.; Bolink, H.J. Perovskite solar cells employing organic charge-transport layers. *Nat. Photonics* **2014**, *8*, 128–132. [CrossRef]
33. Xiao, Z.; Bi, C.; Shao, Y.; Dong, Q.; Wang, Q.; Yuan, Y.; Wang, C.; Gao, Y.; Huang, J. Efficient, high yield perovskite photovoltaic devices grown by interdiffusion of solution-processed precursor stacking layers. *Energy Environ. Sci.* **2014**, *7*, 2619–2623. [CrossRef]
34. Mahmood, K.; Sarwar, S.; Mehran, M.T. Current status of electron transport layers in perovskite solar cells: Materials and properties. *RSC Adv.* **2017**, *7*, 17044–17062. [CrossRef]
35. Chen, G.-S.; Chen, Y.-C.; Lee, C.-T.; Lee, H.-Y. Performance improvement of perovskite solar cells using electron and hole transport layers. *Sol. Energy* **2018**, *174*, 897–900. [CrossRef]
36. Wan, Z.; Xu, M.; Fu, Z.; Li, D.; Mei, A.; Hu, Y.; Rong, Y.; Han, H. Screen printing process control for coating high throughput titanium dioxide films toward printable mesoscopic perovskite solar cells. *Front. Optoelectron.* **2019**, *12*, 344–351. [CrossRef]
37. Chiang, C.-H.; Wu, C.-G. Bulk heterojunction perovskite–PCBM solar cells with high fill factor. *Nat. Photonics* **2016**, *10*, 196–200. [CrossRef]
38. Giordano, F.; Abate, A.; Correa Baena, J.P.; Saliba, M.; Matsui, T.; Im, S.H.; Zakeeruddin, S.M.; Nazeeruddin, M.K.; Hagfeldt, A.; Graetzel, M. Enhanced electronic properties in mesoporous TiO_2 via lithium doping for high-efficiency perovskite solar cells. *Nat. Commun.* **2016**, *7*, 10379. [CrossRef]
39. You, Y.-J.; Saeed, M.A.; Shafian, S.; Kim, J.; Hyeon Kim, S.; Kim, S.H.; Kim, K.; Shim, J.W. Energy recycling under ambient illumination for internet-of-things using metal/oxide/metal-based colorful organic photovoltaics. *Nanotechnology* **2021**, *32*, 465401. [CrossRef]
40. Liang, P.-W.; Liao, C.-Y.; Chueh, C.-C.; Zuo, F.; Williams, S.T.; Xin, X.-K.; Lin, J.; Jen, A.K.Y. Additive Enhanced Crystallization of Solution-Processed Perovskite for Highly Efficient Planar-Heterojunction Solar Cells. *Adv. Mater.* **2014**, *26*, 3748–3754. [CrossRef]
41. Meng, L.; You, J.; Guo, T.-F.; Yang, Y. Recent Advances in the Inverted Planar Structure of Perovskite Solar Cells. *Acc. Chem. Res.* **2016**, *49*, 155–165. [CrossRef]
42. Ranjitha, A.; Thambidurai, M.; Shini, F.; Muthukumarasamy, N.; Velauthapillai, D. Effect of doped TiO_2 film as electron transport layer for inverted organic solar cell. *Mater. Sci. Energy Technol.* **2019**, *2*, 385–388. [CrossRef]
43. Raj, A.; Kumar, M.; Kumar, A.; Laref, A.; Singh, K.; Sharma, S.; Anshul, A. Effect of doping engineering in TiO_2 electron transport layer on photovoltaic performance of perovskite solar cells. *Mater. Lett.* **2022**, *313*, 131692. [CrossRef]
44. Assi, A.A.; Saleh, W.R.; Mohajerani, E. Investigate of TiO_2 and SnO_2 as electron transport layer for perovskite solar cells. *AIP Conf. Proc.* **2020**, *2290*, 050039. [CrossRef]
45. Muthukrishnan, A.P.; Lee, J.; Kim, J.; Kim, C.S.; Jo, S. Low-temperature solution-processed SnO2 electron transport layer modified by oxygen plasma for planar perovskite solar cells. *RSC Adv.* **2022**, *12*, 4883–4890. [CrossRef] [PubMed]
46. Chen, J.; Zhao, X.; Kim, S.-G.; Park, N.-G. Multifunctional Chemical Linker Imidazoleacetic Acid Hydrochloride for 21% Efficient and Stable Planar Perovskite Solar Cells. *Adv. Mater.* **2019**, *31*, 1902902. [CrossRef]
47. Liu, Z.; Deng, K.; Hu, J.; Li, L. Coagulated SnO_2 Colloids for High-Performance Planar Perovskite Solar Cells with Negligible Hysteresis and Improved Stability. *Angew. Chem. Int. Ed.* **2019**, *58*, 11497–11504. [CrossRef]
48. Akin, S. Hysteresis-Free Planar Perovskite Solar Cells with a Breakthrough Efficiency of 22% and Superior Operational Stability over 2000 h. *ACS Appl. Mater. Interfaces* **2019**, *11*, 39998–40005. [CrossRef]
49. Ma, J.; Lin, Z.; Guo, X.; He, J.; Hu, Z.; Su, J.; Zhang, J.; Chang, J.; Hao, Y. Low temperature ZnO/TiOx electron-transport layer processed from aqueous solution for highly efficient and stable planar perovskite solar cells. *Mater. Today Energy* **2019**, *14*, 100351. [CrossRef]
50. Zhang, P.; Wu, J.; Zhang, T.; Wang, Y.; Liu, D.; Chen, H.; Ji, L.; Liu, C.; Ahmad, W.; Chen, Z.D.; et al. Perovskite Solar Cells with ZnO Electron-Transporting Materials. *Adv. Mater.* **2018**, *30*, 1703737. [CrossRef]
51. Gheno, A.; Thu Pham, T.T.; Di Bin, C.; Bouclé, J.; Ratier, B.; Vedraine, S. Printable WO_3 electron transporting layer for perovskite solar cells: Influence on device performance and stability. *Sol. Energy Mater. Sol. Cells* **2017**, *161*, 347–354. [CrossRef]
52. Pang, A.; Shen, D.; Wei, M.; Chen, Z.-N. Highly Efficient Perovskite Solar Cells Based on $Zn_2Ti_3O_8$ Nanoparticles as Electron Transport Material. *ChemSusChem* **2018**, *11*, 424–431. [CrossRef]
53. Sun, C.; Guan, L.; Guo, Y.; Fang, B.; Yang, J.; Duan, H.; Chen, Y.; Li, H.; Liu, H. Ternary oxide $BaSnO_3$ nanoparticles as an efficient electron-transporting layer for planar perovskite solar cells. *J. Alloy. Compd.* **2017**, *722*, 196–206. [CrossRef]
54. Hou, Q.; Ren, J.; Chen, H.; Yang, P.; Shao, Q.; Zhao, M.; Zhao, X.; He, H.; Wang, N.; Luo, Q.; et al. Synergistic Hematite-Fullerene Electron-Extracting Layers for Improved Efficiency and Stability in Perovskite Solar Cells. *ChemElectroChem* **2018**, *5*, 726–731. [CrossRef]

55. Siddiqui, H. Modification of Physical and Chemical Properties of Titanium Dioxide (TiO_2) by Ion Implantation for Dye Sensitized Solar Cells. In *Ion Beam Techniques and Applications*; Intech Open: London, UK, 2019. [CrossRef]
56. Ola, O.; Maroto-Valer, M.M. Review of material design and reactor engineering on TiO_2 photocatalysis for CO2 reduction. *J. Photochem. Photobiol. C Photochem. Rev.* **2015**, *24*, 16–42. [CrossRef]
57. Jung, H.S.; Park, N.-G. Perovskite Solar Cells: From Materials to Devices. *Small* **2015**, *11*, 10–25. [CrossRef]
58. Wali, Q.; Iftikhar, F.J.; Khan, M.E.; Ullah, A.; Iqbal, Y.; Jose, R. Advances in stability of perovskite solar cells. *Org. Electron.* **2020**, *78*, 105590. [CrossRef]
59. Zaky, A.A.; Christopoulos, E.; Gkini, K.; Arfanis, M.K.; Sygellou, L.; Kaltzoglou, A.; Stergiou, A.; Tagmatarchis, N.; Balis, N.; Falaras, P. Enhancing efficiency and decreasing photocatalytic degradation of perovskite solar cells using a hydrophobic copper-modified titania electron transport layer. *Appl. Catal. B Environ.* **2021**, *284*, 119714. [CrossRef]
60. Snaith, H.J.; Abate, A.; Ball, J.M.; Eperon, G.E.; Leijtens, T.; Noel, N.K.; Stranks, S.D.; Wang, J.T.-W.; Wojciechowski, K.; Zhang, W. Anomalous Hysteresis in Perovskite Solar Cells. *J. Phys. Chem. Lett.* **2014**, *5*, 1511–1515. [CrossRef]
61. Wu, M.-C.; Liao, Y.-H.; Chan, S.-H.; Lu, C.-F.; Su, W.-F. Enhancing Organolead Halide Perovskite Solar Cells Performance Through Interfacial Engineering Using Ag-doped TiO_2 Hole Blocking Layer. *Sol. RRL* **2018**, *2*, 1800072. [CrossRef]
62. Gao, X.-X.; Ge, Q.-Q.; Xue, D.-J.; Ding, J.; Ma, J.-Y.; Chen, Y.-X.; Zhang, B.; Feng, Y.; Wan, L.-J.; Hu, J.-S. Tuning the Fermi-level of TiO2 mesoporous layer by lanthanum doping towards efficient perovskite solar cells. *Nanoscale* **2016**, *8*, 16881–16885. [CrossRef]
63. Shallcross, R.C.; Armstrong, N.R. Near-Surface Composition, Structure, and Energetics of TiO_2 Thin Films: Characterization of Stress-Induced Defect States in Oxides Prepared via Chemical Vapor Deposition versus Solution Deposition from Sol–Gel Precursors. *J. Phys. Chem. C* **2021**, *125*, 24011–24024. [CrossRef]
64. Ma, S.; Ahn, J.; Oh, Y.; Kwon, H.-C.; Lee, E.; Kim, K.; Yun, S.-C.; Moon, J. Facile Sol–Gel-Derived Craterlike Dual-Functioning TiO_2 Electron Transport Layer for High-Efficiency Perovskite Solar Cells. *ACS Appl. Mater. Interfaces* **2018**, *10*, 14649–14658. [CrossRef] [PubMed]
65. Kavan, L.; Steier, L.; Grätzel, M. Ultrathin Buffer Layers of SnO_2 by Atomic Layer Deposition: Perfect Blocking Function and Thermal Stability. *J. Phys. Chem. C* **2017**, *121*, 342–350. [CrossRef]
66. Nguyen, M.H.; Yoon, S.-H.; Kim, K.-S. Surface modification of electron transport layers based on TiO_2 nanorod boosts efficiency of perovskite solar cells. *AIChE J.* **2022**, e17958. [CrossRef]
67. Shahvaranfard, F.; Altomare, M.; Hou, Y.; Hejazi, S.; Meng, W.; Osuagwu, B.; Li, N.; Brabec, C.J.; Schmuki, P. Engineering of the Electron Transport Layer/Perovskite Interface in Solar Cells Designed on TiO_2 Rutile Nanorods. *Adv. Funct. Mater.* **2020**, *30*, 1909738. [CrossRef]
68. Song, S.; Kang, G.; Pyeon, L.; Lim, C.; Lee, G.-Y.; Park, T.; Choi, J. Systematically Optimized Bilayered Electron Transport Layer for Highly Efficient Planar Perovskite Solar Cells (η = 21.1%). *ACS Energy Lett.* **2017**, *2*, 2667–2673. [CrossRef]
69. Tavakoli, M.M.; Giordano, F.; Zakeeruddin, S.M.; Grätzel, M. Mesoscopic Oxide Double Layer as Electron Specific Contact for Highly Efficient and UV Stable Perovskite Photovoltaics. *Nano Lett.* **2018**, *18*, 2428–2434. [CrossRef]
70. Hu, W.; Yang, S.; Yang, S. Surface Modification of TiO_2 for Perovskite Solar Cells. *Trends Chem.* **2020**, *2*, 148–162. [CrossRef]
71. Ito, S. Sensitization and Functions of Porous Titanium Dioxide Electrodes in Dye-Sensitized Solar Cells and Organolead Halide Perovskite Solar Cells. In *Perovskite Solar Cells*; Series on Chemistry, Energy and the Environment; World Scientific Publishing Co., Pte. Ltd.: Singapore, 2017; Volume 1, pp. 45–62.
72. Jiang, Q.; Sheng, X.; Li, Y.; Feng, X.; Xu, T. Rutile TiO_2 nanowire-based perovskite solar cells. *Chem. Commun.* **2014**, *50*, 14720–14723. [CrossRef]
73. Chen, X.; Mao, S.S. Titanium Dioxide Nanomaterials: Synthesis, Properties, Modifications, and Applications. *Chem. Rev.* **2007**, *107*, 2891–2959. [CrossRef]
74. Yin, G.; Ma, J.; Jiang, H.; Li, J.; Yang, D.; Gao, F.; Zeng, J.; Liu, Z.; Liu, S.F. Enhancing Efficiency and Stability of Perovskite Solar Cells through Nb-Doping of TiO2 at Low Temperature. *ACS Appl. Mater. Interfaces* **2017**, *9*, 10752–10758. [CrossRef]
75. Singh, T.; Öz, S.; Sasinska, A.; Frohnhoven, R.; Mathur, S.; Miyasaka, T. Sulfate-Assisted Interfacial Engineering for High Yield and Efficiency of Triple Cation Perovskite Solar Cells with Alkali-Doped TiO2 Electron-Transporting Layers. *Adv. Funct. Mater.* **2018**, *28*, 1706287. [CrossRef]
76. Lü, X.; Mou, X.; Wu, J.; Zhang, D.; Zhang, L.; Huang, F.; Xu, F.; Huang, S. Improved-Performance Dye-Sensitized Solar Cells Using Nb-Doped TiO2 Electrodes: Efficient Electron Injection and Transfer. *Adv. Funct. Mater.* **2010**, *20*, 509–515. [CrossRef]
77. Zhang, H.; Shi, J.; Xu, X.; Zhu, L.; Luo, Y.; Li, D.; Meng, Q. Mg-doped TiO_2 boosts the efficiency of planar perovskite solar cells to exceed 19%. *J. Mater. Chem. A* **2016**, *4*, 15383–15389. [CrossRef]
78. Su, T.-S.; Wei, T.-C. Co-Electrodeposition of Sn-Doped TiO_2 Electron-Transporting Layer for Perovskite Solar Cells. *Phys. Status Solidi A* **2020**, *217*, 1900491. [CrossRef]
79. Wu, T.; Zhen, C.; Zhu, H.; Wu, J.; Jia, C.; Wang, L.; Liu, G.; Park, N.-G.; Cheng, H.-M. Gradient Sn-Doped Heteroepitaxial Film of Faceted Rutile TiO_2 as an Electron Selective Layer for Efficient Perovskite Solar Cells. *ACS Appl. Mater. Interfaces* **2019**, *11*, 19638–19646. [CrossRef]
80. Gu, X.; Wang, Y.; Zhang, T.; Liu, D.; Zhang, R.; Zhang, P.; Wu, J.; Chen, Z.D.; Li, S. Enhanced electronic transport in Fe3+-doped TiO2 for high efficiency perovskite solar cells. *J. Mater. Chem. C* **2017**, *5*, 10754–10760. [CrossRef]
81. Xu, Z.; Yin, X.; Guo, Y.; Pu, Y.; He, M. Ru-Doping in TiO_2 electron transport layers of planar heterojunction perovskite solar cells for enhanced performance. *J. Mater. Chem. C* **2018**, *6*, 4746–4752. [CrossRef]

82. Wang, S.; Liu, B.; Zhu, Y.; Ma, Z.; Liu, B.; Miao, X.; Ma, R.; Wang, C. Enhanced performance of TiO_2-based perovskite solar cells with Ru-doped TiO_2 electron transport layer. *Sol. Energy* **2018**, *169*, 335–342. [CrossRef]
83. Arman, S.Y.; Omidvar, H.; Tabaian, S.H.; Sajjadnejad, M.; Fouladvand, S.; Afshar, S. Evaluation of nanostructured S-doped TiO_2 thin films and their photoelectrochemical application as photoanode for corrosion protection of 304 stainless steel. *Surf. Coat. Technol.* **2014**, *251*, 162–169. [CrossRef]
84. Abd Mutalib, M.; Ahmad Ludin, N.; Su'ait, M.S.; Davies, M.; Sepeai, S.; Mat Teridi, M.A.; Mohamad Noh, M.F.; Ibrahim, M.A. Performance-Enhancing Sulfur-Doped TiO_2 Photoanodes for Perovskite Solar Cells. *Appl. Sci.* **2022**, *12*, 429. [CrossRef]
85. Chen, B.-X.; Rao, H.-S.; Li, W.-G.; Xu, Y.-F.; Chen, H.-Y.; Kuang, D.-B.; Su, C.-Y. Achieving high-performance planar perovskite solar cell with Nb-doped TiO_2 compact layer by enhanced electron injection and efficient charge extraction. *J. Mater. Chem. A* **2016**, *4*, 5647–5653. [CrossRef]
86. Lv, M.; Lv, W.; Fang, X.; Sun, P.; Lin, B.; Zhang, S.; Xu, X.; Ding, J.; Yuan, N. Performance enhancement of perovskite solar cells with a modified TiO_2 electron transport layer using Zn-based additives. *RSC Adv.* **2016**, *6*, 35044–35050. [CrossRef]
87. Ranjan, R.; Prakash, A.; Singh, A.; Singh, A.; Garg, A.; Gupta, R.K. Effect of tantalum doping in a TiO_2 compact layer on the performance of planar spiro-OMeTAD free perovskite solar cells. *J. Mater. Chem. A* **2018**, *6*, 1037–1047. [CrossRef]
88. Wang, J.; Qin, M.; Tao, H.; Ke, W.; Chen, Z.; Wan, J.; Qin, P.; Xiong, L.; Lei, H.; Yu, H.; et al. Performance enhancement of perovskite solar cells with Mg-doped TiO_2 compact film as the hole-blocking layer. *Appl. Phys. Lett.* **2015**, *106*, 121104. [CrossRef]
89. Deng, Y.; Li, S.; Li, X.; Wang, R. HI-assisted fabrication of Sn-doping TiO_2 electron transfer layer for air-processed perovskite solar cells with high efficiency and stability. *Sol. Energy Mater. Sol. Cells* **2020**, *215*, 110594. [CrossRef]
90. Koech, R.K.; Ichwani, R.; Oyewole, D.; Kigozi, M.; Amune, D.; Sanni, D.M.; Adeniji, S.; Oyewole, K.; Bello, A.; Ntsoenzok, E.; et al. Tin Oxide Modified Titanium Dioxide as Electron Transport Layer in Formamidinium-Rich Perovskite Solar Cells. *Energies* **2021**, *14*, 7870. [CrossRef]
91. Mulyanti, B.; Wulandari, C.; Hasanah, L.; Pawinanto, R.E.; Hamidah, I. Absorption Performance of Doped TiO_2-Based Perovskite Solar Cell using FDTD Simulation. *Model. Simul. Eng.* **2022**, *2022*, 9299279. [CrossRef]
92. Niu, Y.; Xing, M.; Tian, B.; Zhang, J. Improving the visible light photocatalytic activity of nano-sized titanium dioxide via the synergistic effects between sulfur doping and sulfation. *Appl. Catal. B Environ.* **2012**, *115–116*, 253–260. [CrossRef]
93. Zare Bidaki, A.; Abdizadeh, H.; Pourshaban, E.; Shadabroo, M.S.; Golobostanfard, M.R. Comparing the planar and porous Nb-doped TiO_2 photoanode of triple cation perovskite solar cells. *Mater. Sci. Semicond. Process.* **2022**, *138*, 106259. [CrossRef]
94. Zong, Y.; Zhou, Y.; Zhang, Y.; Li, Z.; Zhang, L.; Ju, M.-G.; Chen, M.; Pang, S.; Zeng, X.C.; Padture, N.P. Continuous Grain-Boundary Functionalization for High-Efficiency Perovskite Solar Cells with Exceptional Stability. *Chem* **2018**, *4*, 1404–1415. [CrossRef]
95. Saidaminov, M.I.; Kim, J.; Jain, A.; Quintero-Bermudez, R.; Tan, H.; Long, G.; Tan, F.; Johnston, A.; Zhao, Y.; Voznyy, O.; et al. Suppression of atomic vacancies via incorporation of isovalent small ions to increase the stability of halide perovskite solar cells in ambient air. *Nat. Energy* **2018**, *3*, 648–654. [CrossRef]
96. Yang, J.-M.; Luo, Y.; Bao, Q.; Li, Y.-Q.; Tang, J.-X. Hall of Fame Article: Recent Advances in Energetics and Stability of Metal Halide Perovskites for Optoelectronic Applications (Adv. Mater. Interfaces 3/2019). *Adv. Mater. Interfaces* **2019**, *6*, 1970017. [CrossRef]

Disclaimer/Publisher's Note: The statements, opinions and data contained in all publications are solely those of the individual author(s) and contributor(s) and not of MDPI and/or the editor(s). MDPI and/or the editor(s) disclaim responsibility for any injury to people or property resulting from any ideas, methods, instructions or products referred to in the content.